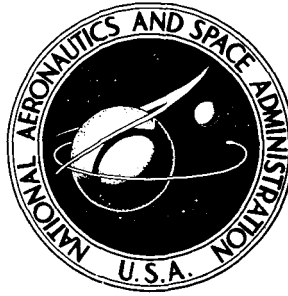


N73-18901

NASA TECHNICAL NOTE



NASA TN D-7084

NASA TN D-7084

APOLLO EXPERIENCE REPORT -  
LUNAR MODULE STRUCTURAL SUBSYSTEM

*by Stanley P. Weiss*

*Manned Spacecraft Center*

*Houston, Texas 77058*

NATIONAL AERONAUTICS AND SPACE ADMINISTRATION • WASHINGTON, D. C. • MARCH 1973

1. Report No. <b>NASA TN D-7084</b>		2. Government Accession No.		3. Recipient's Catalog No.	
4. Title and Subtitle <b>APOLLO EXPERIENCE REPORT LUNAR MODULE STRUCTURAL SUBSYSTEM</b>				5. Report Date <b>March 1973</b>	
				6. Performing Organization Code	
7. Author(s) <b>Stanley P. Weiss, MSC</b>				8. Performing Organization Report No. <b>MSC S-345</b>	
9. Performing Organization Name and Address  <b>Manned Spacecraft Center Houston, Texas 77058</b>				10. Work Unit No. <b>914-13-20-13-72</b>	
				11. Contract or Grant No.	
12. Sponsoring Agency Name and Address  <b>National Aeronautics and Space Administration Washington, D. C. 20546</b>				13. Type of Report and Period Covered <b>Technical Note</b>	
				14. Sponsoring Agency Code	
15. Supplementary Notes  <b>The MSC Director has waived the use of the International System of Units (SI) for this Apollo Experience Report, because, in his judgment, the use of SI units would impair the usefulness of the report or result in excessive cost.</b>					
16. Abstract  <b>In the Apollo Program, the lunar-orbit rendezvous mode was used for the lunar-landing mission. To accomplish the lunar landing, a lunar module spacecraft was built. A description of the design requirements for the structural subsystem and of the structural configuration and the method of design verification are given. A discussion is presented of several problems encountered and the corrective actions taken during the designing, manufacturing, and testing of the lunar module.</b>					
17. Key Words (Suggested by Author(s)) <ul style="list-style-type: none"> <li>• Lunar Module</li> <li>• Ascent Stage</li> <li>• Descent Stage</li> <li>• Structure</li> <li>• Stress Corrosion</li> <li>• Lunar Landing</li> </ul>				18. Distribution Statement	
19. Security Classif. (of this report) <b>None</b>		20. Security Classif. (of this page) <b>None</b>		21. No. of Pages <b>22</b>	
				22. Price <b>\$3.00</b>	

## CONTENTS

Section	Page
SUMMARY . . . . .	1
INTRODUCTION . . . . .	1
GENERAL SUBSYSTEM DESCRIPTION . . . . .	2
Design Requirements . . . . .	2
Configuration Description . . . . .	3
Design Verification . . . . .	5
SIGNIFICANT PROBLEM AREAS . . . . .	5
Descent-Stage Shear-Panel Fatigue and Thickness Control . . . . .	5
Stress Corrosion . . . . .	6
Internally Machined Struts . . . . .	7
Parts Interchangeability . . . . .	8
Lunar-Landing Design Loads . . . . .	9
MISSION PERFORMANCE . . . . .	10
CONCLUDING REMARKS . . . . .	12
APPENDIX A — CONFIGURATION DESCRIPTION . . . . .	13
APPENDIX B — DESIGN VERIFICATION . . . . .	17

## TABLE

Table	Page
I     FLIGHT ANOMALIES . . . . .	11

## FIGURES

Figure	Page
1     Saturn V launch vehicle and payload configuration . . . . .	3
2     Overall LM vehicle configuration . . . . .	3
3     Basic LM dimensions . . . . .	4
4     Lunar module ascent-stage structure . . . . .	4
5     Lunar module descent-stage structure . . . . .	5
6     Typical shear panel showing crack location . . . . .	6
7     Top-deck interim fix . . . . .	6
8     Interchangeable parts on typical beam panel . . . . .	9
A-1   Cross section of a forward window . . . . .	14
A-2   Cross section of the upper docking window . . . . .	15

# APOLLO EXPERIENCE REPORT

## LUNAR MODULE STRUCTURAL SUBSYSTEM

By Stanley P. Weiss  
Manned Spacecraft Center

### SUMMARY

The lunar module spacecraft was designed to operate exclusively in a space environment. A ratio of approximately 1 to 15 of the structural weight to the fully loaded spacecraft weight was achieved. The spacecraft consists of a descent stage and an ascent stage. A clear separation of the stages was accomplished for lunar launch or abort.

The design certification consisted of both component- and vehicle-level tests. Structural problems such as fatigue, stress corrosion, and nonidentical interchangeable parts required changes in the design and manufacture of the lunar module.

No problems were associated with the primary lunar module structure during the 10 Apollo missions, including four lunar landings. The structural anomalies encountered were associated with the secondary structure.

### INTRODUCTION

The lunar module (LM), the first manned spacecraft designed to operate exclusively in a space environment, was required to accomplish the lunar-landing phase of the Apollo Program. The structural subsystem, design requirements, configuration description, design and manufacturing problems, and design verification of the LM are discussed in this paper.

The LM was designed with emphasis on a minimum-weight structure. A typical area in which considerable weight saving was accomplished was in the reduction of structural joints. This reduction was accomplished by machining large structural members instead of machining a number of smaller members and joining them by fasteners. During the design and manufacturing phases, two weight-reduction programs were implemented to remove excess weight from structural members. This weight removal resulted in a ratio of approximately 1 to 15 of the structural weight to the fully loaded spacecraft weight. During the design verification, various design and manufacturing problems were encountered that could be attributed to the actions taken to reduce the weight. Several of the problems encountered and the corrective actions taken are discussed.

The design certification of the structural subsystem of the LM depended primarily on the results of the ground test program, which consisted of both component- and vehicle-level tests. Formal analyses were made to supplement the test program. These analyses served as a baseline and were supplemented by a delta analysis for each mission.

## GENERAL SUBSYSTEM DESCRIPTION

### Design Requirements

The functional design requirements for the LM structural subsystem, which were specified to the contractor in the contract technical specifications, are as follows.

#### 1. Ascent-stage structural subsystem

- a. A pressurized cabin with an allowable leakage rate not to exceed 0.2 pound of oxygen per hour at 5.0 psia in a vacuum
- b. The visibility necessary to enable the crew to perform the basic descent, landing, ascent, rendezvous, and docking maneuvers
- c. Two hatches for crew transfer to and from the command module (CM)
  - (1) Docking or upper hatch for normal crew transfer to and from the CM
  - (2) Front hatch of the LM for egress to and ingress from the lunar surface
  - (3) Both hatches operable from the interior and exterior of the LM
- d. A docking interface and structure compatible with the requirements
- e. Provisions for a structural connection to the descent stage capable of clear separation for lunar launch or abort
- f. Structural support for the life support, environmental control, guidance and navigation, propulsion and stabilization, communications, and electrical power subsystems

#### 2. Descent-stage structural subsystem

- a. Support for the LM in the spacecraft/LM adapter (SLA)
- b. Structural attachment of the LM landing gear
- c. Structural connection to the ascent stage
- d. Structural support for the environmental control, guidance and navigation, propulsion, and electrical power subsystems

- e. Structural support for experiments and equipment for lunar activities
- f. A platform for the lunar-launch ascent or for an abort

## Configuration Description

The launch configuration of the Saturn V and the overall LM vehicle configuration are shown in figures 1 and 2, respectively, and the basic vehicle dimensions are shown in figure 3. Both ascent and descent stages are enclosed in thermal and micrometeoroid shields. A detailed description of the ascent-stage and descent-stage structures is contained in appendix A. Details of the verification and certification of the LM are contained in appendix B.

The ascent-stage structure is divided into three structural areas: crew compartment or cabin, midsection, and aft equipment bay (fig. 4). Aluminum alloys are used primarily in the construction of the ascent stage. The major alloys are 2219 and 7075-T6.

The cabin and midsection structural shell is cylindrical and of semimonocoque construction. The shell is a welded and mechanically fastened assembly of aluminum alloy sheets and machined longerons. The shell is supported by formed sheet-metal

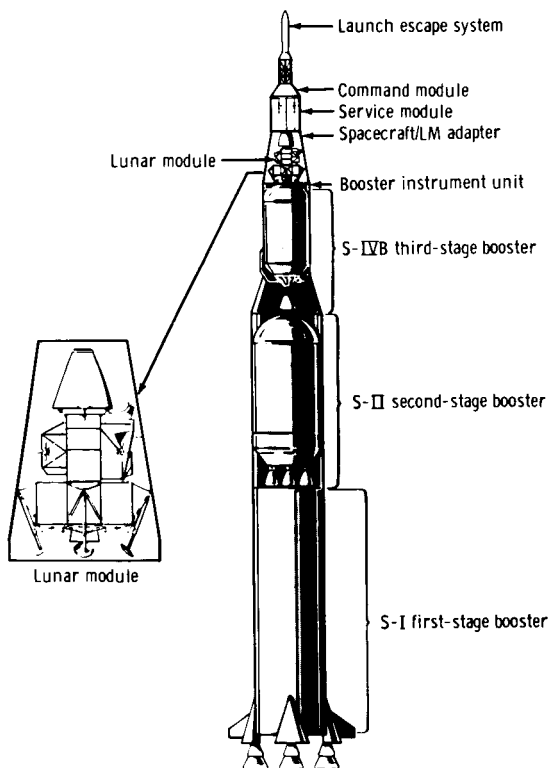


Figure 1. - Saturn V launch vehicle and payload configuration.

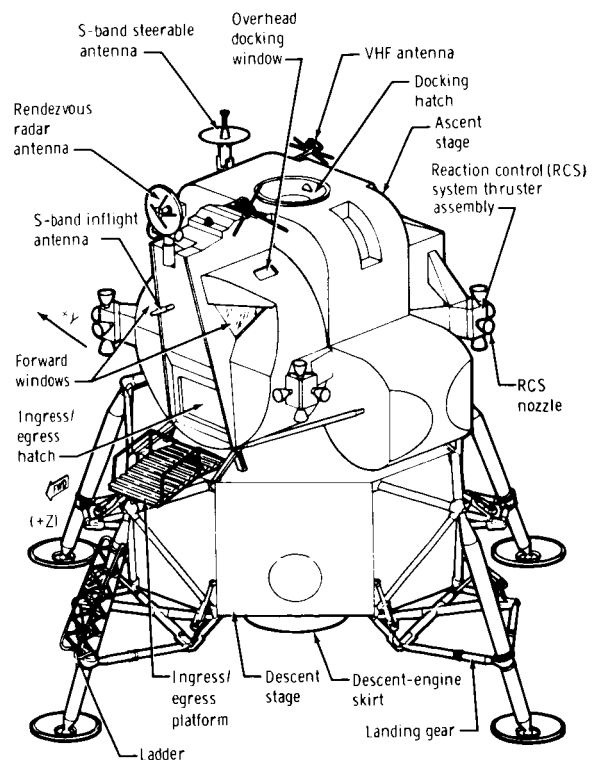


Figure 2. - Overall LM vehicle configuration.

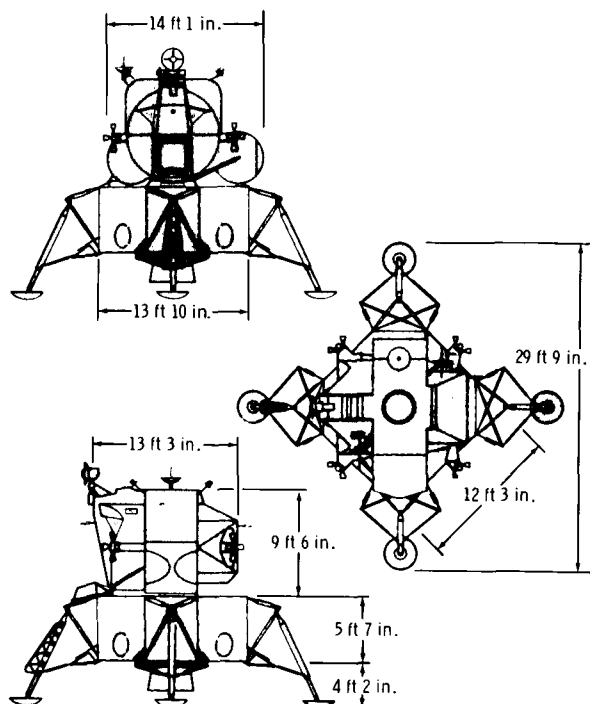


Figure 3. - Basic LM dimensions.

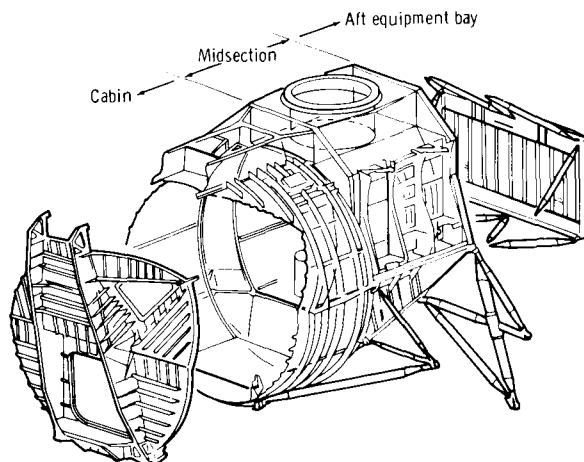


Figure 4. - Lunar module ascent-stage structure.

rings that are riveted to the structural skin. A front-face assembly, attached mechanically to the cabin, encloses the forward end of the cabin. The front-face assembly incorporates openings in the structure for two triangular windows and the egress/ingress hatch. The midsection is attached mechanically to the cabin by a bulkhead. The midsection structure contains an opening for the docking (top) hatch. The aft end of the midsection is closed by a bulkhead. The aft equipment bay is formed by a rack cantilevered off the aft bulkhead by tubular struts. The main propellant tanks are nonintegral and are supported from the midsection by tubular struts. Various other tanks, such as the oxygen and helium tanks, are supported from the aft bulkhead or aft equipment rack in the aft equipment bay.

The descent-stage structure is constructed primarily of chemically milled webs, extruded and milled stiffeners, and milled cap strips (fig. 5). The material used in the construction of the descent stage is primarily 7075-T6 aluminum alloy. Titanium is used where high temperatures are experienced. The main structure consists of two pairs of parallel beams arranged in a cruciform configuration with structural upper and lower decks and end bulkheads. A four-legged truss assembly (outrigger) is attached at the end of each pair of beams. These assemblies serve as support for the LM in the SLA and as attachment points for the main struts of the landing gear (fig. 5).

The five compartments formed by the descent-stage main-beam assemblies house the major components of the propulsion system. The center compartment houses the descent engine, and the four outboard compartments support the nonintegral tanks. The four open quadrant areas of the descent stage are used to support various subsystems equipment and tanks.



## Design Verification

The LM structural design was verified as a result of component- and vehicle-level tests in combination with formal loads and structural analyses. Initially, the certification program consisted primarily of the testing of the LM test article 3 (LTA-3), which was the structural test vehicle. Testing at the component level was conducted when it was impractical to impose the required environment at the vehicle level and only when the correct boundary conditions could be simulated adequately at the component level.

The certification of the LM structural subsystem is defined by a network of certification test requirements. Each certification test requirement (CTR) states the environmental conditions to be imposed during the test, the test-article configuration, and the success criteria for the test. A CTR was written for each test that was required to verify that the design requirements were met.

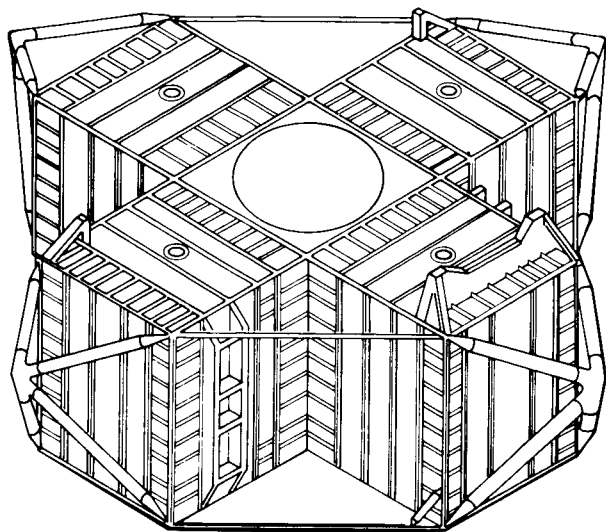


Figure 5. - Lunar module descent-stage structure.

## SIGNIFICANT PROBLEM AREAS

### Descent-Stage Shear-Panel Fatigue and Thickness Control

The descent-stage primary structure is constructed mainly of shear panels that are designed as diagonal-tension field beams. This type of beam develops the required strength after the shear web has developed buckles. The shear panels are chemically milled to provide a minimum-weight structure. The minimum thickness of these panels is 0.006 inch with a chemically milled tolerance of  $\pm 0.002$  inch. During the simulated launch and boost vibration tests, fatigue cracks were noticed at the transition zone between the basic shear web and the rivet land. Typical shear-panel crack locations are shown in figure 6. The diagonal-tension buckle in the shear web terminates at the rivet land with a small radius of curvature that results in a relatively high stress region. The buckle pattern and depth do not change significantly with increasing shear when the web has gone into diagonal tension. An analysis of the test data indicated that the buckles oscillated in the plane of the web. The high stress level was satisfactory from a static viewpoint; however, the low-frequency-vibration environment caused high-stress low-cycle fatigue of the webs. As an interim fix on the early vehicles, a fiber-glass "picture frame" was applied to each panel of the shear deck (three panels per beam) (fig. 7). The layers of fiber-glass cloth were applied in decreasing widths in a pyramidal form to provide a gradual increase in bending stiffness that terminated the buckle

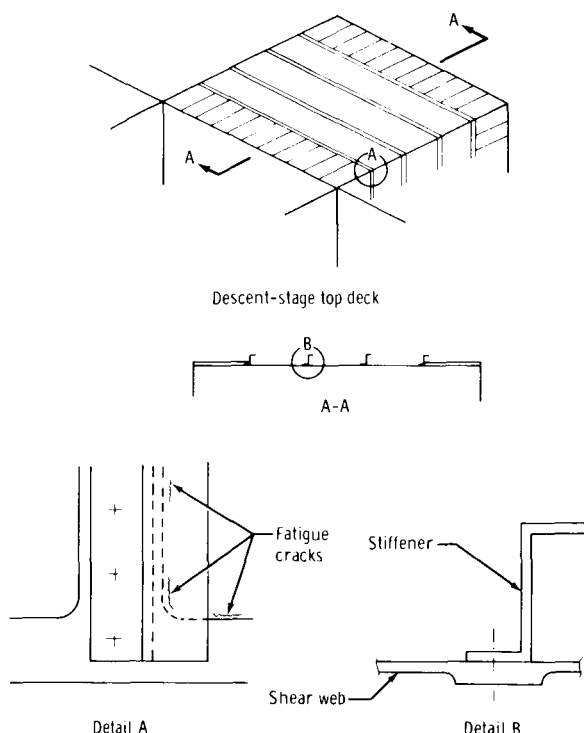


Figure 6. - Typical shear panel showing crack locations.

0.020 inch on the top decks and 0.015 inch on the beam panels and end bulkheads. The effect of the increased thickness was to decrease stress to an acceptable level. The adequacy of the redesign was verified by a vehicle-level test for the launch and boost vibration environments. In a subsequent weight-reduction program, the minimum shear-web thickness for the top decks and beam panels was reduced to 0.015 and 0.012 inch, respectively. This configuration was verified by component panel tests by applying the internal loads determined during the vehicle-level vibration test.

During the time a solution for the fatigue problem was being developed, another problem regarding chemically milled parts was discovered. The thicknesses of the chemically milled webs were not to drawing tolerance, and, in some cases, the webs were found to contain small holes. The control of the thickness of the original sheet of aluminum was inadequate, and, when the sheet was chemically milled, the sheet-thickness variance was duplicated by the chemical milling. When final thicknesses are approximately 0.006 inch, the variance of the sheet-material thickness is extremely important. To correct this problem, a more rigorous process of selecting the sheet material was imposed, and a detailed thickness map was generated for each part after manufacture.

## Stress Corrosion

The first failure attributed to stress-corrosion cracking on the LM structure occurred in October 1966. A fitting on the aft equipment rack failed because of a lack of proper shimming. In November 1967, the LTA-3 aft-equipment-rack support struts

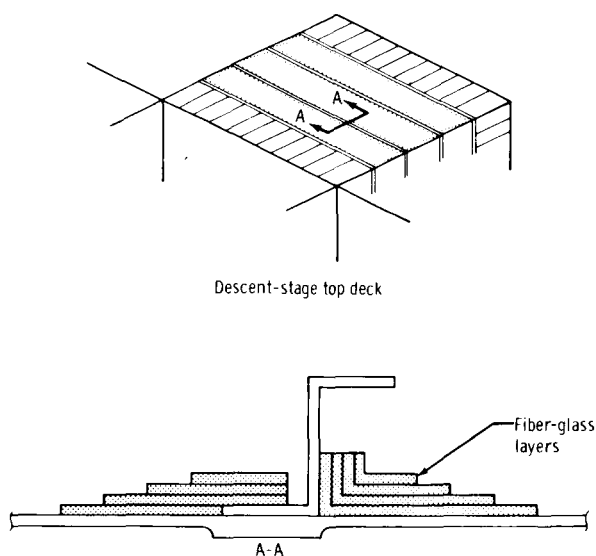


Figure 7. - Top-deck interim fix.

over a longer distance, thereby increasing the radius of curvature. Because the fiber-glass fix was relatively heavy, a redesign of all the shear panels in the descent stage was accomplished to reduce the weight penalty. In the redesign, the minimum web thickness was increased to at least

were being load calibrated in preparation for static structural and drop tests. During the calibration, cracks were discovered on the ends of the swaged tubes where the end fittings were mechanically attached. An extensive investigation of all struts revealed 23 cracked struts in the 264 parts inspected. The failures were attributed to stress corrosion caused by clamp-up stresses induced when the end fittings were attached. The corrective action taken was to modify all struts (64 on the ascent stage and descent stage) for LM-3 and subsequent vehicles. The struts on LM-3 and LM-4 (Apollo missions 9 and 10) were either changed to 7075-T73 if sufficient structural capability existed or modified to provide the required strength, even if stress-corrosion cracking occurred. On each subsequent LM, all struts except the outriggers were redesigned to the 7075-T73 condition. Corrective action on the outriggers consisted of shot peening, liquid shimming, and painting the strut ends. An additional precaution taken on all struts was the use of liquid shim at the attachment of the tube to the end fitting to prevent clamp-up stresses.

The large number of stress-corrosion-induced failures precipitated a review of the entire structure for stress-corrosion-susceptible parts. This review, initiated at the request of the NASA, was conducted in January 1968 with support from the NASA Manned Spacecraft Center (MSC), the NASA Marshall Space Flight Center, the Air Force, and the Navy. The results of the review included an identification of all stress-corrosion-susceptible fittings and initiated an inspection of the fittings judged to be susceptible. Additional corrective actions included changing the heat treatment from 7075-T6 to 7075-T73, providing the required shims, and adding a protective paint to all susceptible fittings on all unassembled vehicles. During the inspections that were conducted as a result of the review, many stress-corrosion cracks were found. The inspections indicated that the problem was chronic throughout the structure. In December 1968, an additional review was conducted to determine which stress-corrosion-sensitive fittings were structurally critical. A structurally critical part was defined as a part that, if cracked in the predicted location, would not meet the required factor of safety. Approximately 40 critical fittings were identified using the data generated during the initial review. The number of fittings varied from vehicle to vehicle, depending on the configuration. The corrective action on the critical fittings consisted of reheattreating to the 7075-T73 condition, redesign using 7075-T73 material, or modification of the existing fitting to provide the required load path, assuming the original fitting was cracked. In addition, liquid shimming applied to the mating surface of all structural members was used to guarantee a perfect match between the parts and to prevent any potential stress-corrosion cracking from clamp-up stresses.

Measures for the prevention of stress corrosion should be included in the design criteria for all spacecraft structures. Stress-corrosion-susceptible alloys (low-threshold alloys such as 7075-T6) should be avoided, whenever practical, to prevent stress-corrosion cracking; and adequate shims, such as liquid shims, should be used.

## Internally Machined Struts

During the static structural test conducted to verify structural adequacy of the LM-10 and subsequent descent stages, failure of a lower outrigger strut occurred. The cause of failure was attributed to an erroneously machined groove on the internal diameter that was not discovered by inspection. The 16 outrigger struts (four per beam) provide the support for the LM in the SLA and for the primary landing-gear

struts. The lower outrigger struts are straight tubular members approximately 53 inches in length, 3.5 inches in diameter, and 0.039 inch in wall thickness and have a closed, integral end fitting. The strut, which is machined from bar stock, must be blind machined the entire length with a varying internal diameter along the length of the strut. The groove that caused the failure was located at the transition from the tube to the end fitting. The type of inspection previously performed was primarily a spot check of the wall thickness. This type of inspection detected only overall discrepancies, not local defects such as grooves. To ensure proper inspection of all struts having a machined internal diameter greater than 2 inches in depth, an inspection technique was developed that used a combination of radiograph and ultrasonic measurements. The radiograph was used primarily to detect localized discontinuities, and the ultrasonic measurements taken on a fine grid were used to determine the wall thickness. The inspections made of assembled vehicles and on-the-shelf items resulted in the identification of approximately 25 structural parts with manufacturing defects, grooves, and undersized wall thicknesses. All the defective parts that resulted in a factor of safety below the acceptable value were either replaced with satisfactory parts of the same design or a modified design. The outrigger struts on LM-10 and subsequent vehicles were replaced with struts with nonintegral end fittings. To preclude the occurrence of a similar anomaly in a highly weight-critical design, particular care should be taken to avoid difficult machining operations. If these operations cannot be avoided, close coordination among engineering, manufacturing, and quality control personnel must be established to ensure adequacy of the finished product.

## Parts Interchangeability

During the inspection of the internally machined struts, parts that were similar in appearance but structurally different were found to be interchanged on the vehicle. In the LM program, considerable emphasis was placed on weight reduction or on keeping weight to a minimum. The emphasis on weight reduction resulted in a design in which many parts were identical except for a few thousandths inch difference in thickness. A detailed review of the entire structure was conducted to determine the parts that were interchangeable. Approximately 2700 parts that could be interchanged were identified. These parts then were reviewed structurally, assuming that the parts were interchanged, to determine if the required factor of safety was maintained. As a result of this review, approximately 260 parts were identified that, if interchanged, would not meet the required factor of safety. These parts were then inspected on all vehicles to verify that the correct part was installed. The type of structural parts that were interchangeable included items such as rod ends, shear clips, cap strips, cap-strip splices, and shear-panel stiffeners. A typical example of the thickness variations in similar parts is shown in figure 8.

The problem of interchangeable parts can be solved by two methods. One method is to key all similar parts to make them noninterchangeable. The other method is to improve the quality control and inspection to ensure manufacture and assembly in accordance with the engineering drawings. The first method will cost weight but is a more reliable way of avoiding incorrect installation of parts; the latter method is lighter but is less reliable.

## Lunar-Landing Design Loads

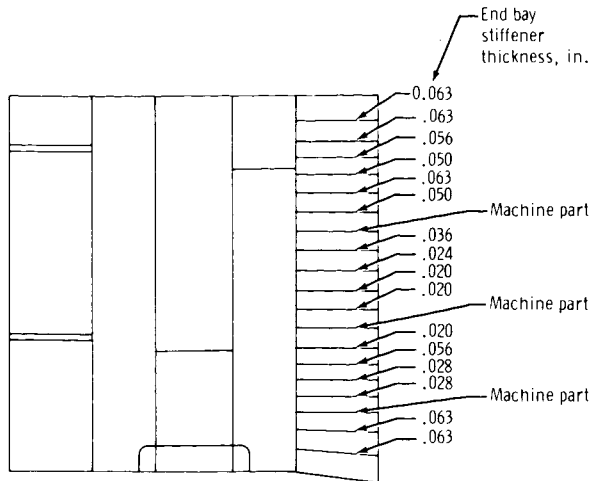


Figure 8. - Interchangeable parts on typical beam panel.

The structural design loads for the lunar-landing condition were based on the consideration of load capability of an individual landing gear, reasonable combinations of individual gear loads, lunar terrain, and the available energy that can be used to stroke the gears to the design position. Each of the four separate landing-gear leg assemblies has energy-absorption capability in the single primary and two secondary struts. The primary strut on each gear leg assembly consists of a lower inner cylinder that fits into an upper outer cylinder. A honeycomb cartridge that fits in the two cylinders provides 9500 pounds of compression stroking at touchdown. The strut is attached at the upper end by a universal

fitting to the descent-stage outrigger assembly. A footpad is attached to the lower end of the inner cylinder by a ball-joint fitting. The secondary struts, two on each landing-gear assembly, also have an inner and an outer cylinder. The secondary struts have a 5000-pound-compression and a 4500-pound-tension stroking capability. The landing-gear design is such that the kinematic position of the footpad can be described by a three-dimensional envelope. Assuming stroking is in the envelope, a unique set of orthogonal loads (X, Y, Z) is required at the landing-gear footpad for equilibrium with the stroking honeycomb cartridges. Structural design loads were chosen from a loads study that considered approximately 30 000 combinations of footpad positions and strut load levels per gear assembly. The stroke-out (100 percent stroking) of the gear honeycomb cartridge was not considered in the loads study. From these loading conditions, 48 cases were judged to provide the most severe structural loading. Using the sets of footpad forces, the vehicle was inertially balanced as a rigid body for each of the 48 load conditions.

To account for the dynamic response of an elastic vehicle to an actual landing, a dynamic magnification factor of 1.6 was applied to the rigid-body loads. The dynamic magnification factor was based on experience with aircraft structures and a judgment of the nature of the dynamic response of the LM structure. An analysis, using an elastic model of the LM, was conducted for a few landing conditions, and the elastic structural response of significant mass items was compared to the rigid-body response. In the cases examined, the load magnification factor did not exceed 1.6.

At this time in the program, weight was an extremely critical issue. In an attempt to reduce structural weight, a variable factor of safety for the 48 cases was generated. Factors of safety of 1.35, 1.15, and 1.0 (rather than the specification requirement of 1.5) were used with the foregoing static-equivalent limit landing loads. A factor of safety of 1.35 was used with the kinematic load sets judged to have the highest possibility of occurrence; a factor of safety of 1.0 was used with the kinematic load sets judged to have very little possibility of occurrence. The use of a maximum factor of safety of 1.35 was acceptable based on the rationale that the landing gear acts as a load-limiting device with respect to the structure. Judgment of the probability of

occurrence of each of the design load cases was made for each kinematic case on the basis of how many gear legs were loaded and the type of load pattern. For example, cases requiring only one gear leg to be under load (in contact with the surface) are likely and, therefore, are assigned a factor of safety of 1.35; however, cases in which all four gear legs are loaded simultaneously and in a complicated manner are extremely unlikely to occur and are assigned a factor of safety of 1.0. The design loads were believed to be conservative; however, because judgment of both contractor and MSC personnel was involved, additional confidence was desired. A detailed Monte Carlo statistical analysis of LM structural response during the lunar-landing phase was conducted by MSC. The study used statistical definitions of lunar-surface conditions obtained from Ranger 8 data and vehicle attitude and velocities obtained from contractor and MSC lunar-landing simulation studies in conjunction with a detailed elastic model of the LM structure and gear. Maximum member loads at critical points throughout the structure were determined for approximately 300 landings. The results of the statistical analysis indicated that the factor of safety of the LM structure was in excess of 1.5 when compared to the resulting 3-sigma loads.

## MISSION PERFORMANCE

The LM structure has been flown on 10 Apollo missions. These missions include the developmental missions that used LTA-2R and LTA-10R and the missions that used LM-1, LM-3, LM-4, LM-5, LM-6, LM-7, LM-8, and LM-10. During these missions, no problems associated with the primary LM structure occurred. Structural anomalies encountered during the missions were associated with the secondary structure. These anomalies and descriptions of the corrective actions are listed in table I. The LTA-2R, LTA-10R, LM-1, and LM-3 were instrumented to obtain data during launch and space flight. The data obtained were used to verify the adequacy of the design environment.

TABLE I. - FLIGHT ANOMALIES

Vehicle	Anomaly	Cause	Action
LM-1	Change in cabin-pressure leak rate	Unknown	None. Minimum cabin pressure was maintained during mission
LM-1	Failure of descent-stage fiber-glass thermal shield	Blanket not fastened adequately	Drawing change assured blanket fastened securely on LM-3
LM-3	Forward hatch binding	Interference with micrometeorite shield and thermal blankets; snubber failed to accommodate floor/hatch spacing	Shield extended and blanket taped for LM-5; snubber also redesigned
LM-3	Descent-stage propellant tank structural contact	Tank contacted upper deck during S-IC engine cut-off	Deck opening enlarged and doubler added for LM-5
LM-3	Docking windows deposits	Contamination from CM waste water and urine	No action required on LM
LM-3	Loose washer between docking window panes	Lack of inspection	Improved inspection
LM-4	LM cabin pressure dropped abruptly at command and service module separation	Pressure on hatch latch (pyrotechnic firing and tunnel pressure) exceeded latch capability; sudden LM decompression followed hatch opening	Undocking procedures changed to ensure low tunnel pressure at LM jettison
LM-4	3.5° misalignment while docked	Command and service module roll jets not disabled after soft docking	Roll jets inhibited during soft dock - vehicles can tolerate required 6° misalignment
LM-5	Cabin decompression required longer than predicted	Cabin pressure transducer reading high on low scale	Time limit established in Apollo Operations Handbook for hatch opening. Removed bacteria filter
LM-6	MESA <sup>a</sup> D-ring handle would not release from support bracket	Possible faulty retention pin or ball; improper pull angle applied to handle for deployment by astronaut	Redesigned handle release mechanism
LM-6	Tear in thermal shield on forward hatch	Damaged during astronaut egress/ingress by portable life support system	Redesigned thermal shield

<sup>a</sup>Modular equipment stowage assembly.

## CONCLUDING REMARKS

The structure of the lunar module has been designed and manufactured to reduce weight to a minimum. The design certification depended primarily on the ground test program. Formal analyses were made to supplement the test program and to serve as a baseline for each mission. Testing at the component level was conducted when it was impractical to impose the required environment at the vehicle level.

Significant problem areas encountered were shear-panel fatigue, thickness control of panels, stress-corrosion cracking, machined-strut tolerances, and interchangeable parts similar in appearance but structurally different.

The structural adequacy of the lunar module to meet the design environment conditions has been verified on 10 Apollo missions. No problems associated with the primary lunar module occurred. The structural anomalies encountered during the mission were associated with the secondary structure and corrective action was taken.

Manned Spacecraft Center  
National Aeronautics and Space Administration  
Houston, Texas, October 2, 1972  
914-13-20-13-72



## APPENDIX A

### CONFIGURATION DESCRIPTION

The overall LM configuration is shown in figure 2, and the basic vehicle dimensions are shown in figure 3. Aluminum alloys are the primary construction material. Some brackets and fasteners are made of titanium. Both the ascent stage and the descent stage are enclosed in thermal and micrometeoroid shields.

### ASCENT STAGE

The ascent-stage structure is divided into three structural areas: cabin, midsection, and aft equipment bay (fig. 4).

The cylindrical structural shell of the cabin is 92 inches in diameter and of semi-monocoque construction. The shell, which is welded and mechanically fastened together, is made of aluminum-alloy sheet metal and machined longerons.

A front-face assembly is attached mechanically to the cylindrical shell, and the construction methods are the same as for the shell. The front-face assembly incorporates openings in the structure for two triangular windows and for the egress/ingress hatch. Two large structural beams, which extend up the forward side of the front-face assembly, are used to carry and to support the structural loads applied to the cabin structure. The lower ends of the beams form and support the two forward interstage fittings; the upper ends of the beams are secured to additional beam structures extending across the top of the cylindrical cabin aft to the midsection structure.

The forward RCS engine clusters are mounted on aluminum-alloy tubular truss members mechanically attached to both sides of the front-face assembly. A truss member extends aft and is secured to a longeron located at the maximum width of the cabin.

The midsection structure consists of a ring-stiffened semimonocoque shell of construction similar to that of the cabin. The midsection is formed by two segments of a cylinder and upper and lower decks. The shell is a chemically milled aluminum skin with machined stiffeners and longerons mechanically attached or welded to it. The cylindrical segments have a radius of 92.0 inches. The upper and lower decks are integrally stiffened machined decks of aluminum alloy that close the midsection. The midsection assembly shell is fastened mechanically to flanges on the two major structural bulkheads. The bulkheads are integrally stiffened machine assemblies of aluminum-alloy plate. The cabin shell is attached mechanically to an outboard flange of the forward bulkhead, which completes the pressurized portion of the ascent stage.

The lower deck of the midsection provides the structural support for the ascent engine. The upper deck provides the structural support for the docking tunnel and hatch. The lower end of the 32-inch-diameter tunnel is welded to the deck structure, and the upper end of the 16-inch-long tunnel is secured to an outer deck. The two main beams running fore and aft, which are integrated with those above the cabin, are secured to the upper deck and support the outboard edge of the outer deck. The aft ends of the

beams are fastened to the aft bulkhead. The aft bulkhead has provisions for bolting the tubular truss members for both aft interstage fittings. The combination of front-face beams, cabin and midsection beams, aft bulkhead, and interstage structure forms a cradle to support the ascent-stage loads. The ascent-engine propellant storage tanks are supported on tubular truss members attached to the forward and aft bulkheads. The RCS propellant-tank-support assemblies are supported externally to both sides of the midsection. Two canted beam assemblies are secured to the bottom of the midsection lower deck and to both fore and aft bulkheads, forming the ascent-engine compartment. The engine-support ring is bolted to the lugs on the lower deck.

The aft equipment bay, located aft of the midsection pressure-tight bulkhead, is an unpressurized area. The supporting structure of the bay consists of tubular truss members bolted to the aft side of the aft bulkhead. The truss members extend from the bulkhead aft to the equipment rack. The equipment-rack assembly is constructed of a series of vertical box beams supported by upper and lower frames. The beams have integral cold plates that serve as a heat-transfer link to the electronic equipment mounted on the beam racks.

Two gaseous oxygen tanks and two helium tanks are secured to truss members and brackets in the area between the aft bulkhead and the equipment rack. Various support mountings and brackets secured to the aft side of the aft bulkhead serve as supports and mounts for valves, plumbing lines, and wiring, and for environmental control system and propulsion subsystems components that do not require a pressurized environment. The two aft RCS thruster clusters are supported by truss members bolted to the upper and lower corners of the equipment-rack assembly and to the aft bulkhead.

The ascent stage is configured with three windows as shown in figure 2. Two triangular windows in the front-face bulkhead of the forward cabin section provide the required visibility during the descent-transfer-orbit, lunar-landing, lunar-stay, and rendezvous phases of the mission. Both windows have approximately 2 square feet of viewing area and are canted down and to the side to permit adequate peripheral and downward visibility. Each window consists of two panes separated from each other by a cavity that is vented to the space environment (fig. A-1). The outer non-structural pane is a micrometeoroid/radiation protective window made from annealed (Vycor) glass. The inner pane is the structural window made from tempered (Chemcor) glass. The outer window is clamped on; the inner window is a "floating" window on a seal constructed from metallic spring surrounded by a Teflon jacket. Both windows on the commander's side (left-hand side) have a landing point designator painted on them that provides the astronaut with the capability to target the desired final landing point.

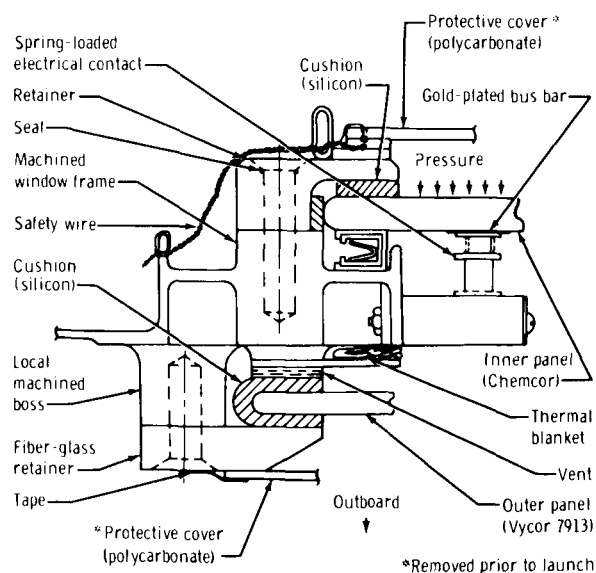


Figure A-1. - Cross section of a forward window.

An overhead docking window on the left side of the vehicle, directly over the commander's head, provides the required visibility during the final phase of the docking maneuver. The docking window has approximately 60 square inches (5 by 12 inches) of viewing area. The construction of this rectangular window (fig. A-2) is similar to that of the two forward windows. One exception is that the inner structural window is not a floating window; it is attached rigidly to the cabin skin by a Kovar edge member bonded to the Chemcor glass and bolted to the cabin structure. Another exception is that the window is curved to match the 92-inch diameter of the cabin skin and is not flat like the forward windows.

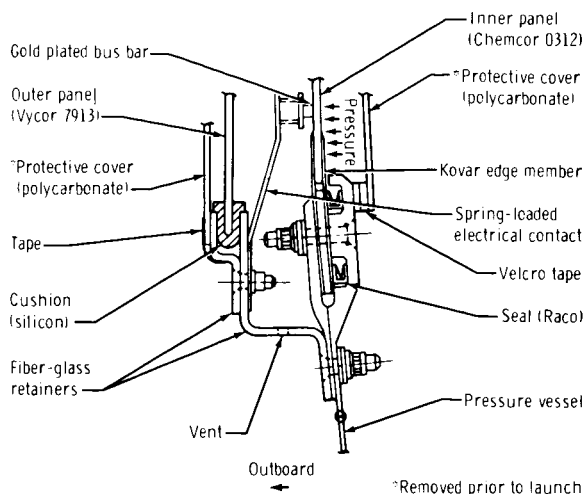


Figure A-2. - Cross section of the upper docking window.

All three inner windows have an electrical conductive coating that is used to heat the window and to remove any moisture (fog or ice) that may accumulate during the mission. The electrical connection, which provides the required power of 115 volts ac for the forward windows and 28 volts dc for the docking window, is a spring-loaded contact against the bus bars that are integral to the glass. The original design required that the electrical wire be soldered directly to the bus bar.

The ascent-stage structure has two hatches (upper and forward) that permit egress/ingress to the LM from both the CM and lunar surface (fig. 2). The upper (docking) hatch is located in the midsection on the +X axis, directly above the ascent-engine cover, and is supported by the upper deck. The hatch is approximately 32 inches in diameter. The forward hatch, located in the forward bulkhead, is a square approximately 32 by 32 inches. Each hatch has hinges on one side and a manually operated single-detent mechanism on the other side that preloads the hatch against the seal. A cabin-pressure-dump-relief valve is located in each hatch. Each hatch is sealed with a preloaded silicon elastomeric-compound seal mounted in the LM structure. When the hatch is closed, a lip near the outer edge of the hatch presses against the seal to ensure a pressure-tight contact. Because both hatches open into the LM, normal cabin pressurization forces the hatches against the seals. To open either hatch, it is necessary to depressurize the cabin through the dump valve.

## DESCENT STAGE

The descent-stage structure is constructed of aluminum alloy, chemically milled webs, extruded and milled stiffeners, and milled cap strips (fig. 5). All joints are fastened with standard mechanical fasteners. The main structure consists of two pairs of parallel beams arranged in a cruciform configuration, with upper and lower decks. The ends of the beams are closed by end-closure bulkheads. A four-legged truss assembly (outrigger) is attached at the end of each pair of beams. These outriggers serve as

support for the LM in the SLA and as the attachment points for the main struts of the landing gear. The truss members are constructed of aluminum-alloy tubing.

The five compartments formed by the descent-stage main-beam assemblies house the major components of the descent propulsion system. The center compartment houses the descent engine supported by eight tubular truss members secured to the four corners of the compartment and to the engine gimbal ring. The two compartments formed on the Z-axis house the oxidizer tanks, and the two compartments formed on the Y-axis house the fuel tanks. The propellant tanks are supported by cylindrical honeycomb skirts attached to the lower decks.

The quadrant areas between the main beams of the descent stage are enclosed, thus giving the stage its octagon shape. These areas use a minimal amount of structure because all components housed in these areas are secured to the main-beam structure. All mounts and brackets that support the components within the quadrant areas are constructed of aluminum-alloy brackets and tubular truss members. The quadrant II area, which supports the scientific equipment and landing radar, is the only area where additional structural support exists. These supports are secured to the main structural-support members.

The descent stage base heat shield (BHS) is subjected to high temperatures of approximately 2400° F maximum caused by radiation from the engine and its plume. The BHS, which protects the descent-stage lower deck, descent propulsion system propellant tanks, and the engine compartment, is a composite of alternate layers of nickel foil and Fiberfrax supported by standoffs attached to the titanium BHS structure.

A specially shaped blast shield of Teflon-coated titanium is secured to the upper edge of the engine compartment, creating an upper deck that covers the entire descent-engine compartment. The shield is used to deflect the ascent-engine plume outward at ignition. The ascent engine is just above and on the same centerline as that of the descent engine.

## APPENDIX B

### DESIGN VERIFICATION

The LTA-3 test program began in January 1966. The test philosophy was to impose the mission environment to the design ultimate conditions in the same sequence that would be experienced during an actual mission.

The test program was initiated with a pressure test of the ascent-stage cabin. This test was conducted to a pressure level of 9.9 psid, 85 percent of design ultimate ( $2.0 \times 5.8$  psid = 11.6). The reduction in the demonstrated factor of safety was necessary to reduce the potential of experiencing a premature failure on the only available test article. If failure had occurred, the required schedule at that time could not have been met. The demonstrated factor of safety during the test program was generally the design factor of safety. For launch load conditions, a reduced demonstrated factor of safety was permitted to the level of the adjacent structure. For example, the SLA factor of safety of 1.4 was permitted. After the successful pressure test, the vehicle was exposed to ascent-engine and descent-engine vibration tests, then shipped to MSC for the launch and boost low-frequency vibration and acoustic tests. These tests were accomplished with the vehicle supported in an SLA. The acoustic test was done with the entire spacecraft; that is, CM, service module, SLA, and LM stacked in the proper configuration. Structural adequacy was verified, and an accurate environment was defined for all LM components and equipment. The data obtained during the two tests provided the qualification environment for all components and verified the adequacy of the environment simulated in the qualification tests already completed.

After the acoustic test, the LTA-3 vehicle was returned to the contractor for continuation of the structural-test program. The static-load tests included conditions that represented the maximum product of dynamic pressure and angle of attack ( $\max q\alpha$ ) and conditions at the end of Saturn V first-stage boost. The  $\max q\alpha$  test was accomplished successfully; however, during the end-boost test, failure of a top-deck shear web occurred at approximately 97 percent of limit load. The failure was a result of fatigue damage accumulated during the previous vibration tests. The vehicle damage incurred during the failure was repaired and the static test continued. At approximately 117 percent of limit load, an upper outrigger strut failed as a result of not having been manufactured according to the engineering requirements. The drawing had been misinterpreted by the shop personnel and inspector. The upper outrigger struts were replaced with correct parts, and the test was continued successfully to 140 percent of limit load.

The next series of vehicle-level tests consisted of static tests to 150 percent of limit load, representing the design conditions on the ascent-engine and descent-engine support structures. Both these tests were completed successfully. The ascent-engine test was repeated successfully when the engine was rotated  $180^\circ$  and canted  $1.5^\circ$  forward to optimize the thrust vector relative to the vehicle center-of-gravity location. As a result, a significant redesign of the support structure was made.

Drop tests were then conducted to verify structural adequacy for lunar landing. The drop tests were different from the static structural tests because the static tests were conducted primarily with the loads applied to the test article by load jacks,

whiffletrees, et cetera. In the drop tests, the objective was to duplicate the kinematic landing loads. A flight set of LM landing gears was used to provide the loads to the vehicle. The gear honeycomb cartridges were precrushed to obtain the landing-gear geometry that would produce the desired kinematic load. This set of forces would provide the desired rigid-body accelerations. The tests were conducted by dropping the LTA-3 from a level position. The landing-gear footpads (nonflight) impacted platforms that were sloped to the required attitude to provide the kinematic load vector. The drop height varied from approximately 8.3 to 42 inches, which provided an impact velocity range of 6.7 to 15 ft/sec. The 15-ft/sec drop exceeded the design requirement for velocity; however, the resulting loads did not exceed design loads. The excess velocity was chosen to provide a longer test duration, which is dependent primarily upon the total energy available at impact. The drop-test program consisted of 16 drops. Six of these were reduced-level drops. The reduced-level drops were accomplished with a special test landing gear that used cartridges with crush characteristics equal to 75 percent of flight-hardware requirements. To demonstrate the capability of the other LM systems to sustain successfully the loads and shock associated with the lunar landing, a series of five drop tests was accomplished on LM-2. These tests were done with all systems operational. Tests and evaluations of the systems both before and after the drop tests indicated that no degradation occurred as a result of the landing shock. The tests were accomplished with the same test equipment used in the structural drop tests. The drop-test series was completed successfully without any test-related problems.

The final series of vehicle-level tests performed on LTA-3 was performed to verify the docking-interface structure. To apply the loads adequately to the LM, a CM structural test article was used that eliminated the necessity of simulating the boundary conditions provided by the CM. The tests were conducted by application of the design loads. After the first docked test, the newly determined mission loads exceeded the design capability as determined by analysis. Additional tests were conducted to determine the actual strength of the design. During the second series, tests were conducted to verify the adequacy by assuming various combinations of failed docking latches. This testing was in support of mission-rules definition. The failed-latch conditions were not original design requirements.

The vehicle-level certification tests were supplemented by component-level tests. Typical areas of the LM structure that were tested by component-level tests were windows, ascent-stage and descent-stage base heat shield, drogue support, hatches, and the modular equipment stowage assembly.